Finite-range simple effective interaction including tensor terms

P. Bano,[1] X. Viñas,[2,3,4] T. R. Routray,[1,*] M. Centelles,[2,3] M. Anguiano,[5] and L. M. Robledo[6,7]

[1]*School of Physics, Sambalpur University, Jyotivihar-768 019, India*

[2]*Departament de Física Quàntica i Astrofísica (FQA), Universitat de Barcelona (UB), Martí i Franquès 1, E-08028 Barcelona, Spain*

[3]*Institut de Ciències del Cosmos (ICCUB), Universitat de Barcelona (UB), Martí i Franquès 1, E-08028 Barcelona, Spain*

[4]*Institut Menorquí d'Estudis, Camí des Castell 28, 07702 Maó, Spain*

[5]*Departamento de Física Atómica, Molecular y Nuclear, Universidad de Granada, E-18071 Granada, Spain*

[6]*Departamento de Física Teórica and CIAFF, Universidad Autónoma de Madrid, E-28049 Madrid, Spain*

[7]*Center for Computational Simulation, Universidad Politécnica de Madrid, Campus de Montegancedo, Boadilla del Monte, 28660-Madrid, Spain*

(Received 13 June 2022; accepted 5 August 2022; published 15 August 2022)

An existing parametrization of the simple effective interaction (SEI) that is able to reproduce the experimentally known crossing between the $2p_{3/2}$ and $1f_{5/2}$ single-particle (s.p.) proton levels in neutron-rich Ni isotopes has been generalized. We have added a short-range tensor force in order to describe the observed gaps between the $1h_{11/2}$ and $1g_{7/2}$ s.p. proton levels in the Sn isotopic chain and between the $1i_{13/2}$ and $1h_{9/2}$ s.p. neutron levels in $N = 82$ isotones without compromising the good agreement with the splittings in the Ni isotopes. Different scenarios where tensor effects are relevant are considered with the new interaction and its predictions are compared with results from other mean-field models and experimental data where available.

DOI: 10.1103/PhysRevC.106.024313

I. INTRODUCTION

Modern experimental facilities such as SPIRAL at GANIL, ISOLDE at CERN, FAIR at GSI, and FRIB at MSU are delivering many new data about properties of exotic nuclei near the drip lines. These experiments have revealed many unexpected phenomena, especially in nuclei far from the stability valley. Among them, the changes that appear in the nuclear shell structure, such as, for instance, the disappearance of the standard magic neutron numbers $N = 20$ and 28 and the emergence of new ones such as $N = 14$, 16, 32, or 34 [1–11], are of special relevance. All these new scenarios represent an excellent testing ground for different nuclear models available in the literature and give the opportunity to improve them in order to better describe the physics of exotic nuclei. For instance, there are several examples scattered over the nuclear chart where the plain mean-field description using effective forces is unable to describe correctly the pattern of the energy gaps between certain s.p. energy levels along isotopic and isotonic chains [12–14]. In the last two decades it has been observed that the inclusion of the tensor contribution to the nucleon-nucleon (NN) interaction is helpful towards describing several of the shell effects just mentioned [15–17]. The relevance of the tensor part of the NN interaction was early established in explaining the nonvanishing quadrupole moment of the deuteron [18,19]. However, due to its limited role in several nuclear phenomena, it has not been usually taken into account in studies based on effective forces of Skyrme and Gogny type. But as new data have poured in with the advent of radioactive ion beam facilities, the exploration of the role of the tensor part of the NN interaction in the mean-field model calculations has regained interest.

In recent years a new type of effective interaction, denoted "simple effective interaction" (SEI), has been developed and applied to the description of different properties of finite nuclei [20,21]. The form of this interaction is quite similar to that of Gogny or Skyrme forces, but what makes it different is the fact that its fitting protocol strongly differs from the usual ones. As a consequence some of the typical deficiencies of Gogny or Skyrme forces are not observed in SEI. An example of this is the crossing between the $2p_{3/2}$ and $1f_{5/2}$ s.p. proton levels in neutron-rich Ni isotopes and the magicity of the atomic number $Z = 28$ in this isotopic chain, which is a subject of current interest from both, experimental and theoretical points of view [22,23]. As shown recently [24], this crossing can be reproduced by SEI at a pure mean field level, while the Skyrme forces SIII and SAMi-T require a short-range momentum-dependent tensor part to reproduce the crossing of the aforementioned levels at the right mass number [25,26]. The reproduction of this crossing by the Gogny force D1M also requires an additional finite-range tensor force, as shown in the Hartree-Fock (HF) calculation in coordinate space performed by Anguiano *et al.* [27–29]. Alternatively, adding a short-range tensor part as the one used in Skyrme forces to Gogny D1M and in the framework of the quasi-local density functional theory [30,31] the crossing is also reproduced [24]. On the other hand, it is important to note that the inclusion of a tensor force on top of an effective interaction does not guarantee the reproduction of the $1f_{5/2}$ and $2p_{3/2}$ s.p. proton levels crossing in neutron-rich Ni isotopes. A typical example is the situation with the Skyrme interaction SLy5, which includes explicitly a tensor contribution in the fitting procedure

*Corresponding author: trr1@rediffmail.com

[14] but is unable to reproduce the above-mentioned proton level crossing in Ni, as is shown in Fig. 1 of Ref. [24]. This results shows the relevance of the underlying central mean-field in determining the position and gaps of the s.p. energy levels and diminishes the importance of tensor terms.

In this paper we show that the addition of a short-range tensor force to SEI is required in order to reproduce the trends of the observed gaps between the $1h_{11/2}$ and $1g_{7/2}$ s.p. proton levels in the Sn isotopic chain and between the $1i_{13/2}$ and $1h_{9/2}$ s.p. neutron levels in the $N = 82$ isotones and that this can be achieved without spoiling the good agreement with the splittings in the Ni isotopes.

The paper is organized as follows: In the second section we revise the basic aspects of the mean-field approach based on the SEI, paying special attention to the fitting protocol of its parameters, in order to show the reason for the difference found between SEI and other effective interactions of Skyrme or Gogny types. In the same section, the short-range tensor force used in this work is briefly discussed. The third section is devoted to discuss the predictions of the SEI at a pure mean-field level in some relevant scenarios of neutron-rich nuclei. Next, using the SEI supplemented by a short-range tensor force we analyze the gaps between the $1h_{11/2}$-$1g_{7/2}$ s.p. proton levels along the Sn isotopic chain and between the $1i_{13/2}$-$1h_{9/2}$ s.p. neutron levels in isotones of $N = 82$. A comparison with the corresponding results provided by a selected set of Skyrme and Gogny forces is also carried out. In the last section, a summary of the results obtained and some concluding remarks are given.

II. FORMALISM

A. The simple effective interaction

The SEI was introduced in Ref. [32] by Behera and collaborators in a way that closely resembles the Gogny force but with one of the ranges set to zero (i.e., a contact term). Its explicit form in coordinate space is given by

$$\begin{aligned} V_{\text{eff}} &= t_0(1 + x_0P_\sigma)\delta(\mathbf{r}) \\ &+ \frac{t_3}{6}(1 + x_3P_\sigma)\left(\frac{\rho(\mathbf{R})}{1 + b\rho(\mathbf{R})}\right)^\gamma \delta(\mathbf{r}) \\ &+ (W + BP_\sigma - HP_\tau - MP_\sigma P_\tau)e^{-r^2/\alpha^2} \\ &+ iW_0\,\vec{\nabla}\,\delta(\mathbf{r}) \times \vec{\nabla} \cdot \vec{\sigma}. \end{aligned} \tag{1}$$

Ten parameters of this interaction, namely, α, γ, b, x_0, x_3, t_3, W, B, H, and M, are fit to reproduce nuclear matter (NM) properties. The two remaining parameters, i.e., the strengths of the zero-range force t_0 and the spin-orbit (SO) interaction W_0 are determined from finite nuclei calculations. The protocol adopted for the parameter determination in case of SEI is somewhat different from the one adopted for other effective forces due to the fact that the momentum and density dependence of the mean fields properties in NM of different types has to satisfy certain experimental and empirical conditions. More specifically the following conditions are imposed:

(1) The mean field in symmetric nuclear matter (SNM) should change sign at a kinetic energy of the incident nucleon of 300 MeV. This constraint is justified by the analysis of the heavy-ion collision (HIC) data at intermediate energies [33–36].
(2) The entropy in pure neutron matter (PNM) should not exceed that of SNM [37].
(3) The effective-mass splitting in spin polarized neutron matter should follow, as close as possible, the behavior of the Dirac-Bruckner-Hartree-Fock (DBHF) calculation using the Bonn-B potential [38].
(4) The density dependence of the isospin asymmetric part of the equation of state (EoS) should be fixed from the standard value of the saturation properties supplemented by the empirical condition that the asymmetric nucleonic contribution in β-stable charge neutral $n + p + e + \mu$ matter must be a maximum.
(5) The stiffness of the SNM EOS is determined by the exponent γ of the density dependent t_3 term.

Typically, γ is used as a free parameter that is in the range of values for which the pressure-density relation remains within the allowed range extracted from the analysis of the HIC data at intermediate energies [39]. The upper limit of $\gamma \approx 1$ thus corresponds to a maximum value of the incompressibility of $K = 283$ MeV. Other γ values used in this work, namely, $\frac{1}{6}$, $\frac{1}{3}$, $\frac{1}{2}$, and $\frac{2}{3}$ correspond to SNM incompressibility values of 207, 226, 246, and 263 MeV, respectively.

The density-dependent term is also modified with a denominator containing the parameter b. This denominator is introduced to prevent supraluminous effects in NM [40]. With the parameters determined by this fitting protocol, the SEI is able to reasonably reproduce the trends of the EoS and the momentum dependence of the mean-field properties obtained in microscopic calculations of NM [37,41–44]. The parameter t_0 together with the SO strength W_0 are fixed by fitting the binding energies (BEs) of the magic nuclei ^{40}Ca and ^{208}Pb.

In the present study, finite nuclei are described by using the so-called quasi-local density functional theory (QLDFT). The QLDFT is a kind of HF calculation where the nonlocal exchange contribution is written as a local density functional by using the extended Thomas-Fermi approximation including up to second-order terms in the $\hbar$ expansion of the density matrix [30,31]. The HF equations become Schrödinger-like coupled equations for the s.p. wave functions,

$$\left[-\boldsymbol{\nabla} \cdot \frac{\hbar^2}{2m_q^*}\boldsymbol{\nabla} + U_q(\mathbf{R}) - \mathbf{W}_q(\mathbf{R})(\boldsymbol{\nabla} \times \boldsymbol{\sigma})\right]\phi_q = \epsilon_q\phi_q, \tag{2}$$

where the subscript $q = n, p$ indicates the type of particle, m_q^* represents the effective mass, U_q is the mean-field experienced by the nucleon of type q, $\mathbf{W}_q$ is the form factor of the spin-orbit potential, and ϵ_q is the s.p. energy corresponding to the orbital ϕ_q. This set of equations, which are local in coordinate space, can be solved in the case of spherical symmetry in a similar way to that used for Skyrme forces. The excellent agreement between the predictions for spherical nuclei obtained using the QLDFT approximation and the full HF results including exchange terms has been discussed in detail in Ref. [21]. To deal with pairing correlations in open-shell

TABLE I. The twelve parameters for the SEI-G ($\gamma = 0.42$) along with the nuclear matter saturation properties (such as saturation density ρ_0, energy per nucleon $e(\rho_0)$, incompressibility for symmetric nuclear matter K, effective mass m^*/m, symmetry energy E_s, slope of symmetry energy L, and curvature of the symmetry energy $K_{\rm sym}$.

γ	b (fm^3)	α (fm)	ε_{ex} (MeV)
0.42	0.5050	0.7591	−95.0536
ε^l_{ex} (MeV)	ε_0 (MeV)	ε^l_0 (MeV)	ε_γ (MeV)
−63.3691	−91.6562	−53.1272	90.0035
ε^l_γ (MeV)	t_0 (MeV fm^3)	x_0	W_0 (MeV fm^5)
65.3966	341.2	1.7933	113.4
Nuclear matter saturation properties			
ρ_0 (fm^{-3})	$e(\rho_0)$ (MeV)	K (MeV)	m^*/m
0.1584	−16.0	240	0.711
E_s (MeV)	L (MeV)	K_{sym} (MeV)	
35.5	76.71	−155.0	

nuclei, we use the Bardeen-Copper-Schrieffer (BCS) approach together with a zero-range density-dependent pairing interaction of the type proposed by Bertsch and Esbensen. The strength is fit to reproduce the pairing gaps in NM predicted by the Gogny interactions [20,21].

By the reasons discussed below we mainly use in this work the SEI EoS corresponding to $\gamma = 0.42$. The twelve parameters of this interaction along with the saturation properties in NM are given in Table I.

B. The spin-orbit force and the tensor force

To describe finite nuclei with SEI a zero-range SO interaction similar to that used in Skyrme and Gogny interactions is added. The corresponding contribution to the energy density is given by

$$\mathcal{H}_{\rm SO} = -\frac{W_0}{2}[\rho\nabla\cdot\mathbf{J} + \rho_n\nabla\cdot\mathbf{J}_n + \rho_p\nabla\cdot\mathbf{J}_p], \tag{3}$$

where the spin-orbit densities $\mathbf{J}_q$ ($q = n, p$) read

$$\mathbf{J}_q(\mathbf{r}) = \frac{1}{4\pi r^3}\sum_i v_i^2(2j_i+1) \times\left[j_i(j_i+1) - l_i(l_i+1) - \frac{3}{4}\right]R_i^2(r). \tag{4}$$

The sum index i runs over all the quantum numbers labeled by $i = n, l, j$, $R_i(r)$ is the radial part of the wave function, and v_i is the BCS occupation probability of each state. The contribution to the SO potential is obtained from the variation of $H_{\rm SO}$ with respect to $\mathbf{J}_q$, $q = n, p$, which results in

$$\mathbf{W}_q = \frac{W_0}{2}(2\nabla\rho_q + \nabla\rho_{q'}). \tag{5}$$

In this work, a short-range tensor term similar to the one used in the case of Skyrme interactions is added to SEI. The reason to use a short-range tensor is that we have checked previously [24] in the case of the Gogny D1M force that a QLDFT calculation including a short-range tensor force provides a finite nuclei description extremely close to the one obtained in full HF calculations with a finite-range tensor [27–29]. The similarity between SEI and Gogny D1M gives us confidence on a similar property for SEI. Although the contribution of the short-range tensor force to the energy density functional has been discussed in detail in earlier literature [14,25], we briefly summarize it here for a sake of completeness.

The short-range tensor force used in this work includes triplet-even and triplet-odd terms, with strengths T and U, respectively. Its explicit form is

$$\begin{aligned} V_T = \frac{T}{2}\Big\{&[(\boldsymbol{\sigma}_1\cdot\mathbf{k}')(\boldsymbol{\sigma}_2\cdot\mathbf{k}') - \frac{1}{3}(\boldsymbol{\sigma}_1\cdot\boldsymbol{\sigma}_2)\mathbf{k}'^2]\delta(\mathbf{r_1}-\mathbf{r_2}) \\ &+ \delta(\mathbf{r_1}-\mathbf{r_2})[(\boldsymbol{\sigma}_1\cdot\mathbf{k})(\boldsymbol{\sigma}_2\cdot\mathbf{k}) - \frac{1}{3}(\boldsymbol{\sigma}_1\cdot\boldsymbol{\sigma}_2)\mathbf{k}^2]\Big\} \\ &+ U\Big\{(\boldsymbol{\sigma}_1\cdot\mathbf{k}')\delta(\mathbf{r_1}-\mathbf{r_2})(\boldsymbol{\sigma}_2\cdot\mathbf{k}) \\ &- \frac{1}{3}(\boldsymbol{\sigma}_1\cdot\boldsymbol{\sigma}_2)[\mathbf{k}'\delta(\mathbf{r_1}-\mathbf{r_2})\mathbf{k}]\Big\}, \end{aligned} \tag{6}$$

where $\mathbf{k} = (\nabla_1 - \nabla_2)/2i$ acts on the right and $\mathbf{k}' = -(\nabla_1 - \nabla_2)/2i$ on the left. In the case of Skyrme forces, the tensor interactions contribute to both the mean-field and spin-orbit potentials owing to their dependence on the neutron and proton spin densities $\mathbf{J}_n$ and $\mathbf{J}_p$, respectively [14,25]. However, in the case of SEI or the Gogny interaction the spin densities only appear in the spin-orbit energy density within the QLDFT formalism. Therefore the tensor term only modifies the spin-orbit part of the energy density. As we are using a short-range tensor interaction, the associate energy density reads [14,25]

$$\mathcal{H}_T = \tfrac{1}{2}\alpha_T\left[\mathbf{J}_n^2 + \mathbf{J}_p^2\right] + \beta_T\mathbf{J}_n\mathbf{J}_p, \tag{7}$$

where the coefficients α_T and β_T are related to the tensor strengths by

$$\alpha_T = \tfrac{5}{12}U, \quad \beta_T = \tfrac{5}{24}(T+U). \tag{8}$$

As a consequence, the spin-orbit form factor is modified by the tensor force and reads

$$\mathbf{W}_q = \frac{W_0}{2}(2\nabla\rho_q + \nabla\rho_{q'}) + \alpha_T\mathbf{J}_q + \beta_T\mathbf{J}_{q'}. \tag{9}$$

III. RESULTS AND DISCUSSION

A. Simple effective interaction predictions for exotic neutron-rich nuclei

At this point, it is worthwhile to recall several predictions of the SEI for neutron-rich nuclei, some of them reported in more detail in earlier literature. Let us mention that the SEI, in spite of being a nonrelativistic model without an isovector contribution in the spin-orbit sector, is able to reproduce the experimental kink of the isotopic shift of the charge radius in the Pb isotopic chain for neutron number $N = 126$ [20]. The ground-state deformation properties and the fission barriers predicted by SEI are analyzed in Ref. [45], finding a good agreement with the accepted experimental values [46].

TABLE II. Ni nuclei ground-state energy for $A = 68$ to 78 calculated for the four EoSs of the SEI compared with experimental values [47].

Nuclei	SEI ($\gamma = \frac{1}{6}$) E (MeV)	SEI ($\gamma = \frac{1}{3}$) E (MeV)	SEI ($\gamma = \frac{1}{2}$) E (MeV)	SEI ($\gamma = \frac{2}{3}$) E (MeV)	Expt. [47] E (MeV)
^{68}Ni	−591.60	−591.08	−590.37	−590.46	−590.407
^{70}Ni	−604.76	−604.52	−603.80	−603.82	−602.300
^{72}Ni	−616.44	−616.32	−615.73	−615.83	−613.455
^{74}Ni	−627.04	−627.03	−626.49	−626.71	−623.820
^{76}Ni	−636.64	−636.75	−636.27	−636.53	−633.156
^{78}Ni	−645.81	−645.38	−644.96	−645.27	−641.550

A region of particular interest from both experimental and theoretical points of view is around magic numbers $Z = 28$ and $N = 50$. We briefly summarize here the SEI predictions in this region [24]. A significant feature of the neutron-rich Ni isotopes is the crossing between the $2p_{3/2}$ and $1f_{5/2}$ s.p. proton levels, which takes place for the nucleus ^{74}Ni. This is a direct consequence of the spin inversion from $3/2^-$ to $5/2^-$ that takes place beyond ^{73}Cu and which has been recently confirmed experimentally [22,23]. We have reexamined this level crossing of Ni isotopes in Ref. [24] by comparing SEI predictions with the results provided by different mean-field models of Skyrme and Gogny types. It is found that, for the SEI, the crossing is reproduced in a natural way without including any additional tensor term that is otherwise required in the case of the Skyrme and Gogny interactions.

We report in Table II the binding energies (BEs) of Ni isotopes from $A = 68$ to $A = 78$ computed at QLDFT level for four equations of state (EoSs) of the SEI, corresponding to the γ values $\frac{1}{6}$, $\frac{1}{3}$, $\frac{1}{2}$, and $\frac{2}{3}$ and including pairing correlations at BCS level, along with the experimental values. Calculations performed with these SEI EoSs reveal that the crossing between the $2p_{3/2}$ and $1f_{5/2}$ s.p. levels moves towards higher mass numbers for smaller values of the γ parameter (i.e., of the incompressibility modulus), as can be seen in Fig. 1. The neutron s.p. levels close to the Fermi energy obtained using SEI with different γ values are displayed in Fig. 2. We see that the gap between the $2d_{5/2}$ and $1g_{9/2}$ s.p. levels remains almost stationary as one moves from ^{68}Ni to ^{78}Ni, which implies that the magicity of the $N = 50$ neutron number is preserved.

Very recently, measurements of charge radii $R_{\rm ch}$ in $Z = 28$ isotopes have been made [48], which allow us to perform comparisons between experimental values and theoretical predictions of the charge radii in all light-mass isotopic chains from $Z = 19$ to $Z = 50$. The charge radii $R_{\rm ch}$ and the isotopic shifts $\delta\langle R^2_{\rm ch}\rangle$ with respect to the nucleus ^{60}Ni computed with the SEI EoS with $\gamma = 0.42$ of Ni isotopes from ^{58}Ni to ^{70}Ni are displayed in Figs. 3 and 4 together with the experimental data extracted using collinear laser spectroscopy [48]. The charge radii predicted by SEI are in good agreement with the experiment and show a similar quality as predicted by the *ab initio* calculations using the NNLO$_{\rm sat}$ potential [48] as well as with the values obtained with the SLy5-T Skyrme interaction. However, charge radii in this region are overestimated by the SAMi-T [26] and SIII-T [49] interactions. The isotopic shifts of the charge radii with respect to the ^{60}Ni nucleus are particularly well reproduced by SEI on the average. In comparison, the SLy5-T and SIII-T predictions overestimate the isotopic shift for isotopes heavier than ^{64}Ni, whereas SAMi-T fails in reproducing the absolute values of the charge radii as well as the trends of the experimental isotopic shifts in the considered Ni isotopes.

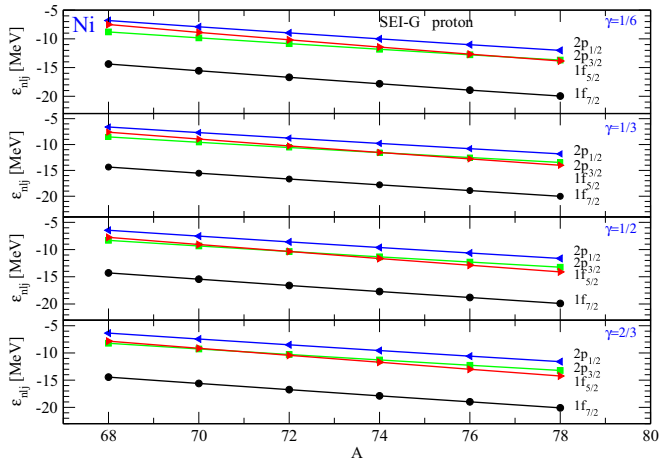

FIG. 1. Proton single-particle levels around the Fermi level for Ni isotopes from $A = 68$ to $A = 78$ computed with the SEI for the four EoSs.

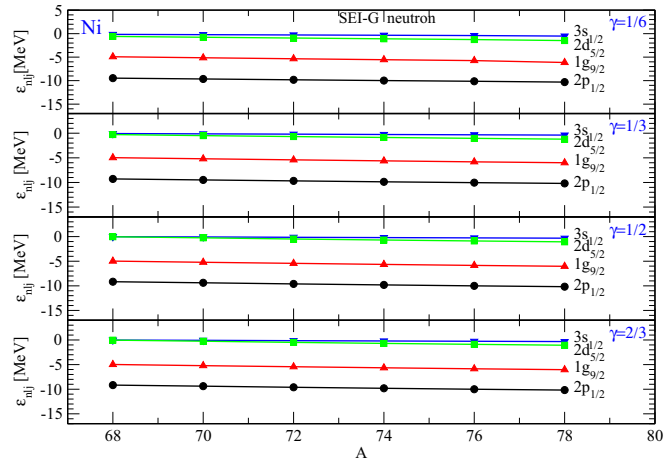

FIG. 2. Neutron single-particle levels around the Fermi level for Ni isotopes from $A = 68$ to $A = 78$ computed with the SEI for the four EoSs.

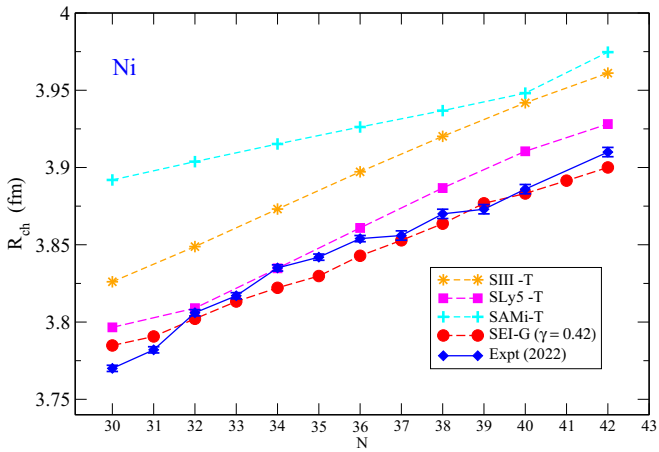

FIG. 3. Nuclear charge radii $R_{\rm ch}$ of Ni isotopes using SEI-G ($\gamma = 0.42$) compared with the experimental data [48].

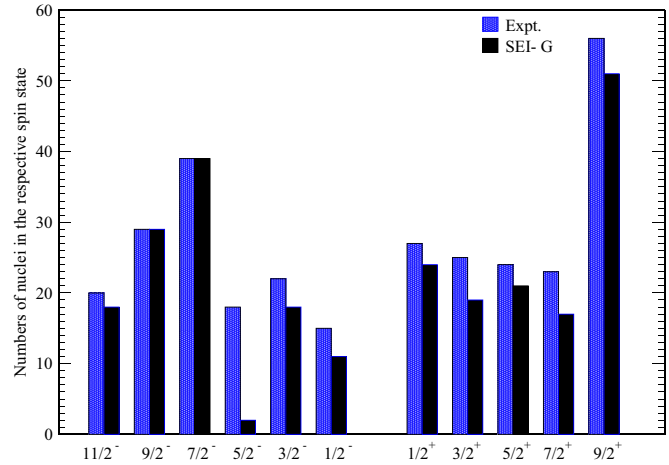

FIG. 5. Comparison of experimental [47] and SEI-G ($\gamma = 0.42$) spins of 298 odd-nuclei in different spin states.

Odd spherical nuclei and the Cu case

Experimental data on the s.p. energy levels in Ni isotopes is not very abundant and often one has to recourse to information extracted from the studies in Co, Zn, and Cu isotopes. In recent γ-spectroscopic studies of Cu-isotopes [22,23], it has been found that the inversion of the ground-state spin-parity from $3/2^-$ to $5/2^-$ occurs at neutron number $N = 46$, which suggests the crossing of $2p_{3/2}$ and $1f_{5/2}$ s.p. proton levels in the underlying Ni core. This experimental scenario for Cu isotopes can be theoretically reproduced with SEI. One possible reason for this success is the good description of spherical odd nuclei with SEI at the QLDFT level and using the uniform blocking method of Ref. [50]. The ground-state spin and parity of 298 spherical odd-nuclei computed with the EOS of SEI with $\gamma = 0.42$ are displayed in Fig. 5. More than 80% of the ground state's spin-parity experimental data is reproduced in our approach. This is similar to the performance of the compilation of spins performed in Ref. [51] based on the results provided by several Skyrme forces and the finite-range droplet model of Möller. To investigate the inversion of the spin-parity in Cu isotopes with our model, we have calculated the energy of the ground and several excited states, assumed of s.p. nature, of Cu-isotopes in the mass number region $A = 69$–79 assuming spherical symmetry for all the considered nuclei because the deformation in these neutron-rich Cu-isotopes is rather small [52]. We have studied the inversion of ground-state spin-parity from $3/2^-$ to $5/2^-$ in Cu isotopes for the SEI EoS with γ values between $\frac{1}{6}$ and $\frac{2}{3}$. We find that, for $\gamma = 0.42$, this inversion of the spin-parity of the ground state occurs at $N = 46$, in agreement with the experimental results [22,23]. The ground-state energies and spin-parity of the Cu-isotopes together with their first excited-state energies obtained with this γ value are collected in Table III. This γ value corresponds to an incompressibility $K(\rho_0) = 240$ MeV, which conforms to the range 240 ± 20 MeV extracted from the compressional mode of vibration in finite nuclei [53] and the ranges obtained from related studies of the giant monopole resonance and heavy-ion collisions [54–57].

This EoS also predicts reasonably well the energy of the first-excited state, as can also be seen in the same Table III. The calculated energies of the first-excited states in other Cu-isotopes in this chain also compares well with the experimental results, which are taken from Fig. 2 of Ref. [22]. For example, the nucleus ^{75}Cu described by this EoS of SEI predicts the energy of excited state $3/2^-$ at 103 keV, whereas the experimental value is 62 keV.

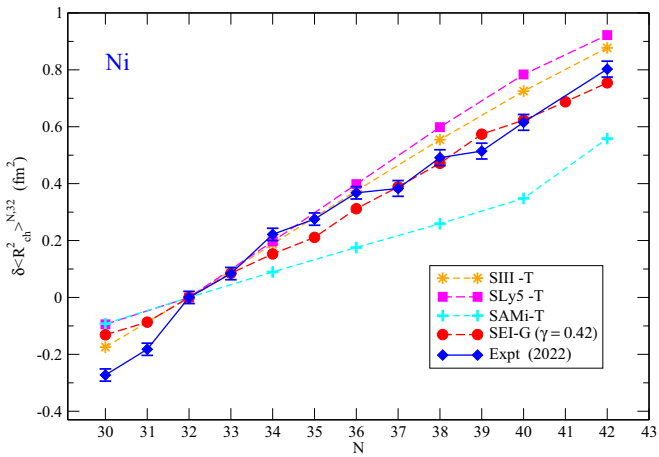

FIG. 4. Isotopic shift $\delta\langle R^2_{\rm ch}\rangle$, with respect to ^{60}Ni, of Ni isotopes using SEI-G ($\gamma = 0.42$) compared with the experimental data [48].

B. Simple effective interaction with a short-range tensor force

In spite of the success of SEI in describing some exotic scenarios of neutron-rich nuclei at the mean-field level by means of QLDFT calculations, as we have discussed in the previous section, there are other particular situations where the mean-field description alone is not able to reproduce, even qualitatively, the experimental data and the addition of a tensor force on top of SEI becomes mandatory.

In this section we analyze first the energy gaps between the $1h_{11/2}$-$1g_{7/2}$ s.p. proton levels in the $Z = 50$ isotopic chain and between the $1i_{13/2}$-$1h_{9/2}$ s.p. neutron levels in the $N = 82$

TABLE III. Ground-state spin and energy of neutron-rich odd Cu isotopes predicted by the SEI EoS ($\gamma = 0.42$). The energy of the first-excited state E^* is also given along with the experimental results taken from Ref. [22].

Nucleus	Spin-parity	SEI ($\gamma = 0.42$) Energy (MeV)	Expt. Energy (MeV)	SEI ($\gamma = 0.42$) E^* (keV)	Expt. E^* (keV)
^{69}Cu	3/2−	−599.40	−599.97	663	1215
^{71}Cu	3/2−	−613.73	−613.09	449	537
^{73}Cu	3/2−	−626.51	−625.51	156	263
^{75}Cu	5/2−	−638.25	−637.13	103	62
^{77}Cu	5/2−	−649.11	−647.42	292	295
^{79}Cu	5/2−	−658.94	−656.65	620	660

isotonic chain comparing with the available experimental data [12] as well as with the predictions of other mean-field models such as the SIII and SAMI-T Skyrme forces and the D1MTd Gogny interaction. Another example where a tensor interaction on top of the SEI is needed is the study of the evolution of the $1h_{11/2}$, $1g_{7/2}$, $2d_{3/2}$, and $2d_{5/2}$ s.p. neutron levels in the $N = 51$ isotonic chain, where the results obtained with our model are compared with the behavior predicted by Federman and Pittel [58].

To get a better agreement with the results reported in Ref. [12], we add to SEI a short-range tensor interaction, which depends on the neutron and proton spin densities [see Eq. (7)]. Its main effect is to modify the spin-orbit potential Eq. (9) and therefore to change the relative position of the neutron and proton s.p. energy levels. The parameters T and U of the tensor force are chosen to describe the energy gaps given in Ref. [12] under the constraint that the crossing of $2p_{3/2}$ and $1f_{5/2}$ s.p. levels in Ni isotopes at neutron number $N = 46$ remains unchanged. For each pair of T and U values, the spin-orbit strength W_0 is readjusted to reproduce the experimental BE of ^{208}Pb. We have found that the tensor force with strength parameters $T = 800$ MeV, $U = -140$ MeV and a spin-orbit strength $W_0 = 122$ MeV fm^5 fulfills these requirements. This procedure for determining the tensor parameters T and U is different from the strategy used in Ref. [49], where they are fit to reproduce the spectra of ^{48}Ca and ^{56}Ni. We have checked that the spin-orbit splittings of these two nuclei computed within our approach give quite similar results to those displayed in Figs. 1 and 2 of Ref. [49].

With the values $T = 800$ MeV and $U = -140$ MeV of the tensor parameters, the $1h_{11/2}$-$1g_{7/2}$ proton gap in even Sn isotopes and the $1i_{13/2}$-$1h_{9/2}$ neutron gap in $N = 82$ isotones are qualitatively reproduced compared with the results of Schiffer *et al.* [12]. The results for these proton and neutron gaps, with and without including the tensor force, are displayed in Figs. 6 and 7, respectively. In the same figures we show the results predicted by the Skyrme forces SIII, SLy5 and SAMi-T, the Gogny force D1MTd as well as the experimental data of Ref. [12]. To enlighten the influence of the tensor force on the relative change of the gaps between the aforementioned s.p. levels, the theoretical results are shifted so that the predicted splittings for the spin-saturated ^{132}Sn nucleus, in both the cases, coincide with the corresponding experimental values.

As explained in detail in Ref. [16], the tensor force provides an additional attraction between neutron and proton particle or hole states with spins $j_> = l + 1/2$ and $j'_< = l' - 1/2$ (or with $j_< = l - 1/2$ and $j'_> = l' + 1/2$) and repulsion with spins $j_> = l + 1/2$ and $j'_> = l' + 1/2$ (or with $j_< = l - 1/2$ and $j'_< = l' - 1/2$). These tensor interactions are stronger between states with similar radial wave functions, i.e., with the same principal quantum number and the same orbital angular momentum because in this case there is a large overlap along the radial directions.

Proton gaps in the $Z = 50$ isotopic chains and neutron gaps in the $N = 82$ and $N = 51$ isotonic chain

The tensor effects on the gap between the unoccupied $1h_{11/2} - 1g_{7/2}$ proton states along the Sn isotopic chain strongly depend on the position and occupancy of the neutron s.p. levels, which in the case of the SEI are displayed in Figs. 8 and 9, respectively. We see from Fig. 8 that, as mentioned, the impact of the tensor force is more important for states of large orbital angular momentum, such as $1g_{7/2}$ or $1h_{11/2}$, whose s.p. energies are clearly shifted with respect to the values computed without the tensor interaction. The tensor force does not act on the $3s_{1/2}$ state, and its effect on the $2d_{5/2}$ and $2d_{3/2}$ states is small due to their small angular momentum. From the same figure we can also see that, above $N = 50$, the neutron levels $1g_{7/2}$ and $2d_{5/2}$ predicted by SEI lie very

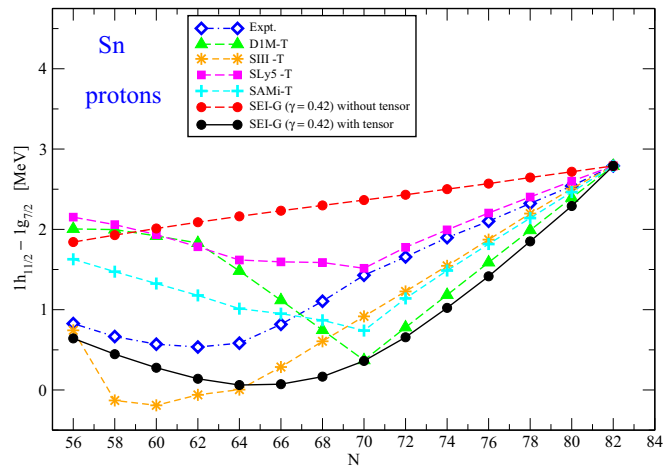

FIG. 6. Energy differences between $1h_{11/2}$ and $1g_{7/2}$ proton s.p.levels in Sn isotopes with and without the tensor interaction. The experimental data are taken from Ref. [12]. For details see the text.

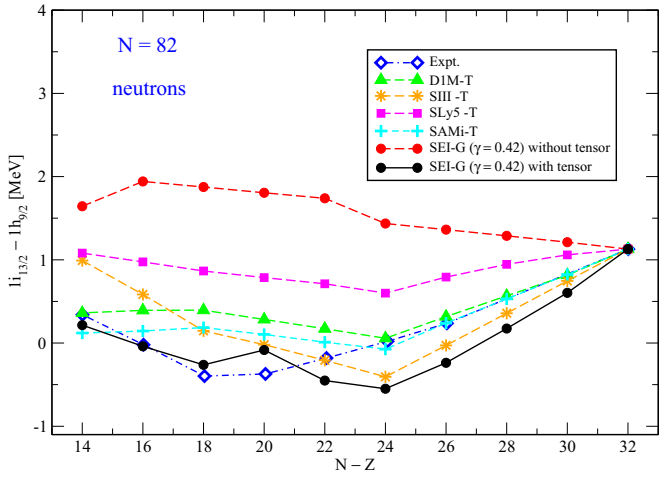

FIG. 7. Energy differences between $1i_{13/2}$ and $1h_{9/2}$ neutron s.p. levels in $N = 82$ computed with and without tensor interaction. The experimental data are taken from Ref. [12]. For details see the text.

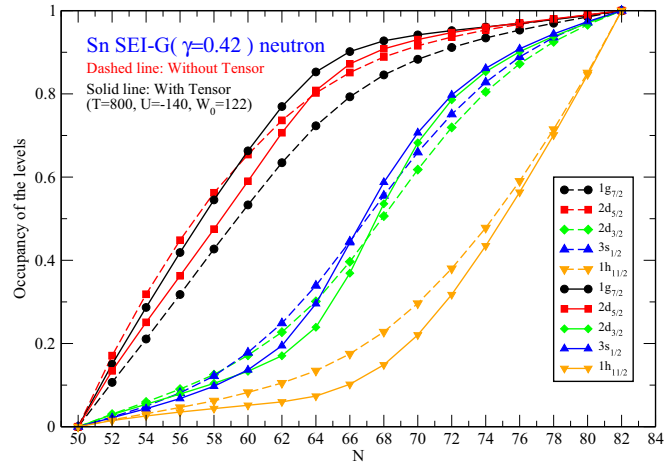

FIG. 9. Occupation probability of the neutron levels of the Sn isotopes in the $N = 50$ to $N = 82$ major shell. Solid (dashed) lines correspond to the occupations computed with (without) the tensor force.

close to each other. The same happens with the $3s_{1/2}$ and $2d_{3/2}$ levels, while the $1h_{11/2}$ level remains rather isolated at higher s.p. energy. As can be seen from Fig. 9, from $A = 100$ to $A = 114$, neutrons in the Sn isotopic chain mainly populate the $1g_{7/2}$ and $2d_{5/2}$ levels almost with the same occupation probability, which reaches 80% at $A = 114$. Above this mass number the occupancy of the $3s_{1/2}$ and $2d_{3/2}$ levels increases remarkably until about 60% in competition with the filling of the $1h_{11/2}$ level, which has a small occupation up to $A = 120$, but from this mass number on increases until saturating at $A = 132$.

The filling of the $1g_{7/2}$ neutron state above $N = 50$ enhances the splittings in the h and g s.p. proton states due to the tensor interaction, thereby decreasing the gap between the $1h_{11/2}$ and the $1g_{7/2}$ proton levels. The effect of filling of the $2d_{5/2}$ neutron level on these two previously mentioned proton levels is just the opposite. Since the occupancy of the $1g_{7/2}$ and $2d_{5/2}$ s.p. neutron levels is quite similar (see Fig. 9), there is a partial cancellation between their tensor effects. This is because the overlap between the s.p. wave functions of the states $1g_{7/2}$ (neutrons) and $1h_{11/2}$ or $1g_{7/2}$ (protons) is larger than the overlap corresponding to the neutron state $2d_{5/2}$ and these proton states. Thus the SEI calculation including the tensor force predicts that the $1h_{11/2} - 1g_{7/2}$ proton gap decreases when the mass number A increases from 100 to 114, which is in agreement with the experimental data [12].

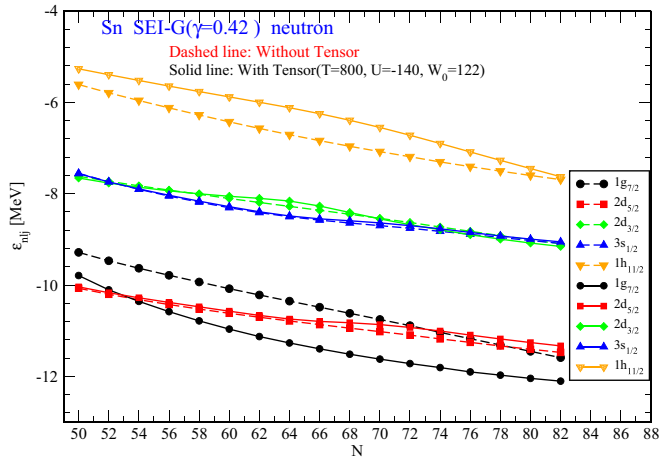

FIG. 8. Neutron levels of Sn isotopes in the $N = 50$ to $N = 82$ major shell. Solid (dashed) lines correspond to the s.p. energies computed with (without) the tensor force.

When the mass number of the isotope increases above $A = 114$, the occupancy of the $2d_{3/2}$ and $3s_{1/2}$ neutron levels becomes progressively important, as can be seen in Fig. 9. The tensor interaction between the $2d_{3/2}$ neutron state and the $1h_{11/2}$ and $1g_{7/2}$ proton states should decrease the proton gap. However, this effect is almost canceled out by the opposite contribution of the $2d_{5/2}$ neutron state. As a consequence the SEI prediction in the $A = 114$–120 range is an almost flat proton gap compared with the experimental increasing trend when the mass number A is above 114 [12]. The calculation with SEI including tensor terms recovers this increasing trend at $A = 120$ owing to the growing occupancy of the $1h_{11/2}$ neutron level (see Fig. 9), which enhances the attraction on the $1g_{7/2}$ and the repulsion on the $1h_{11/2}$ proton levels increasing thus the gap between these two states.

Similar effects due to the tensor force can be seen in the evolution of the relative separation of the unoccupied $1i_{13/2}$ and $1h_{9/2}$ neutron levels in the isotones of $N = 82$ in Fig. 7. For this isotonic chain the evolution of the proton s.p. levels in the $Z = 50$–72 major shell and their corresponding occupancies as a function of the atomic number are displayed in Figs. 10 and 11, respectively. As the proton number increases from $Z = 50$ to $Z = 58$, the $1g_{7/2}$ proton level fills up until practically saturating at $Z = 58$. Due to the tensor force, this proton level pulls the $1i_{13/2}$ and push the $1h_{9/2}$ neutron levels decreasing the gap between them. From $Z = 58$ to $Z = 64$, again only the $2d_{5/2}$ proton level fills up appreciably (see Fig. 11), but in this case the tensor force acts in the opposite

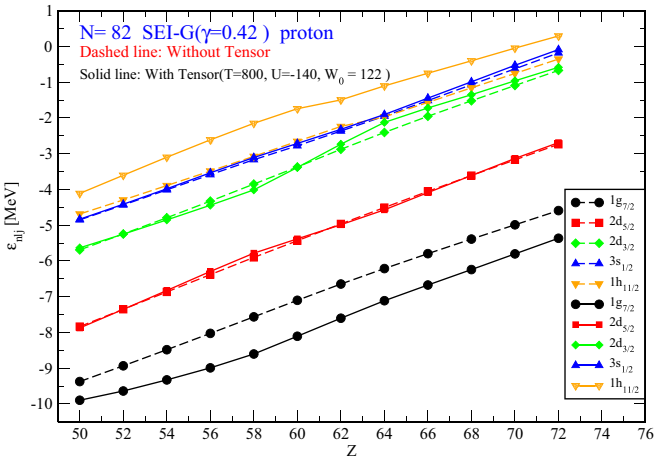

FIG. 10. Proton levels of the $N = 82$ isotones in the $Z = 50$ to $Z = 72$ major shell. Solid (dashed) lines correspond to the s.p. energies computed with (without) the tensor force.

way, i.e., it pushes up the $1i_{13/2}$ and pulls down the $1h_{9/2}$ neutron levels, increasing the $1i_{13/2}$–$1h_{9/2}$ neutron gap. The kink at $Z = 62$ is due to the increasing of the occupancy of the $2d_{3/2}$ proton level, which becomes prevalent to compensate the increase of the gap due to the $2d_{5/2}$ level. Beyond $Z = 64$ and up to $Z = 70$, the situation in the case of SEI with $\gamma = 0.42$ is more complicated because the $2d_{3/2}$, $3s_{1/2}$, and $1h_{11/2}$ proton levels are almost degenerate and they populate simultaneously, as can be seen in Fig. 11. In this region the reduction of the $1i_{13/2}$-$1h_{9/2}$ neutron gap due to the $2d_{3/2}$ proton level is compensated by the increasing effect of the $1h_{11/2}$ proton level, whose wave function has larger overlap with the wave functions of the neutron levels because of the same principal quantum number and similar orbital angular momentum.

It can be seen from Fig. 6 that if the tensor force is absent the SEI model predicts an almost linear smooth growing

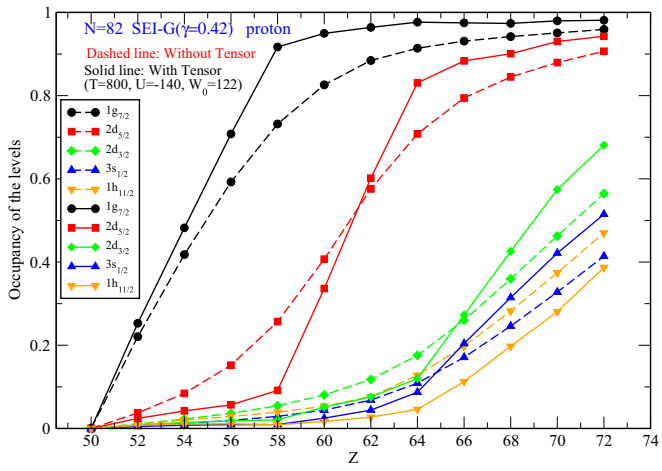

FIG. 11. Occupation probability of the proton levels of the $N = 82$ isotones in the $Z = 50$ to $Z = 72$ major shell. Solid (dashed) lines correspond to the occupations computed with (without) the tensor force.

tendency as a function of the neutron number, which is in disagreement with the experimental results reported in Ref. [12]. As we have seen, the trends of the experimental results are much better reproduced by adding to SEI a short-range tensor interaction discussed in this work. Also, the behavior of the experimental gaps between the $1i_{13/2}$ and $1h_{9/2}$ neutron levels in the $N = 82$ isotopic chain is better reproduced by the theoretical calculations performed with SEI when the tensor force is included in the calculation as can be seen in Fig. 7. This improvement of the theoretical predictions with respect to the experiment is due to the fact that the tensor force modifies the position of the underlying s.p. energy levels provided by the mean field and therefore changes the gaps among the levels from a rather uniform value when tensor interaction is absent to a more oscillating structure of the gaps due to the tensor effects when the consecutive s.p. orbits are filled.

We have also analyzed the role of the pairing correlations in the theoretical calculation of the proton and neutron gaps in Sn isotopic and $N = 82$ isotonic chains in the particular case of the SIII Skyrme force. Although the behavior of the gaps is mainly ruled by the effects of the tensor interaction on the s.p. energy levels, the BCS occupancies of the s.p. energy levels may modify the tensor effects, as far as the tensor force acts simultaneously on different levels around the Fermi energy. This is just the situation for isotopes of Sn in the range $N = 64$–70 because in this case the $2d_{3/2}$ and $3s_{1/2}$ neutron s.p. levels, which are almost degenerate, lie below the $1h_{11/2}$ s.p. neutron level that is empty if pairing correlations are absent but partially occupied when pairing acts, and therefore modify the $1h_{11/2}$-$1g_{7/2}$ proton gap with respect to the case without pairing. On the contrary, in isotones of $N = 82$ pairing correlations are almost marginal in the neutron gaps predicted by the SIII force, because in this case the $2d_{3/2}$ and $3s_{1/2}$ s.p. proton levels are above the $1h_{11/2}$ s.p. proton level, and therefore they do not contribute to the $1i_{13/2}$-$1h_{9/2}$ neutron gap in the range of atomic numbers $Z = 64$–70 if pairing is absent. When the pairing interaction is switched on, the $2d_{3/2}$ s.p. neutron level contributes to the change of the aforementioned neutron gaps, but its effect is very small and does not change the trend due to the tensor interaction of the slightly less occupied $1h_{11/2}$ proton level. We have found in our calculations that a similar result is obtained when comparing results by using the Gogny interactions D1M and D1MTd. In general, the tensor interaction reduces the pairing correlations [59].

In the same Figs. 6 and 7 we have displayed the $1h_{11/2}$-$1g_{7/2}$ proton and $1i_{13/2}$-$1h_{9/2}$ neutron gaps in the Sn isotopic chain and $N = 82$ isotonic chain computed with other mean-field models of Skyrme and Gogny types, as mentioned before. The tensor effects in these models are qualitatively the same as those discussed for the SEI, but quantitatively they depend on the strength of the tensor force used as well as on the energies and occupancies of the s.p. levels in each considered model. We see that the relative tensor effects computed with different interactions reproduce fairly well the experimental results of Ref. [12] within a window of about 1 MeV for both the isotopic chain of Sn and the isotonic chain of $N = 82$. However, from a quantitative point of view, these proton and neutron gaps computed with the different mean-field models

TABLE IV. Shifts in MeV applied to the $1h_{11/2}$-$1g_{7/2}$ proton gaps in the Sn isotopic chain and to the $1i_{13/2}$-$1h_{9/2}$ neutron gaps in the $N = 82$ isotonic chain for the different models considered in this work (see text for further explanations).

	SEI	SEI-T	SIII-T	SLy5-T	SAMi-T	D1M-T
$1h_{11/2} - 1g_{7/2}$	1.85	2.99	2.12	0.35	4.00	3.00
$1i_{13/2} - 1h_{9/2}$	0.90	1.16	0.57	−0.31	3.29	1.45

show larger differences with respect to the values reported in Ref. [12]. This is due to the underlying mean-field effects, which are different from the small changes induced by the tensor force, and determine the absolute position of the s.p. energy levels. The values of the shifts applied to the $1h_{11/2}$-$1g_{7/2}$ proton gaps and $1i_{13/2}$-$1h_{9/2}$ neutron gaps using the different mean-field models considered in this work are reported in Table IV.

The SEI model plus the tensor force used in this work is also able to reproduce the experimental trends of the evolution of the $1h_{11/2}$, $1g_{7/2}$, and $2d_{3/2}$ neutron s.p. levels in the $N = 51$ isotonic chain. As Z increases from 41 to 50, filling the $1g_{9/2}$ proton level, the $1h_{11/2}$ neutron s.p. level is pushed up while the $1g_{7/2}$ and the $2d_{3/2}$ s.p. neutron levels are pulled down owing to the tensor interaction as compared with the case where the tensor force is absent. The lowering of the $1g_{7/2}$ neutron level is a phenomenon pointed out by Federman and Pittel [58]. These effects are shown in Fig. 12, where the evolution of these s.p. neutron levels relative to the $2d_{5/2}$ neutron level are shown for the cases without and with the tensor force. From this figure we can see that the lowering of the $1g_{7/2}$ level along this chain is more prominent, as expected, than the one experienced by the $2d_{3/2}$ level, owing to the larger overlap of the wave function of the $1g_{9/2}$ proton level with the one of the $1g_{7/2}$ neutron level as compared with the overlap with the wave function of the $2d_{3/2}$ neutron level, which has different principal quantum number and angular momentum.

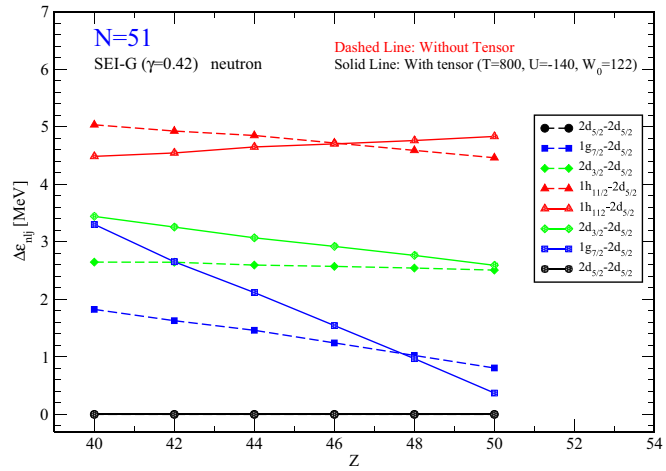

FIG. 12. Neutron s.p. levels in $N = 51$ isotones relative to the $2d_{5/2}$ level with and without tensor interaction.

IV. CONCLUSIONS

The main aim of this work is to study the impact of an additional tensor force on different predictions of the SEI model at mean field level. To this end we have used the SEI parametrization with $\gamma = 0.42$, which was fit in a recent work [24] to describe the crossing between the $2p_{3/2}$ and $1f_{5/2}$ s.p. proton levels in neutron-rich Ni isotopes at mass number $A = 74$ (or the spin-parity inversion of the ground-state of Cu-isotopes measured experimentally in the nucleus ^{75}Cu [22,23]). We have chosen a short-range tensor interaction similar to that used in Skyrme forces. Subject to the constraint that the above-discussed predictions for Ni- and Cu-isotopes are not violated, the two strength parameters T and U of the tensor part have been adjusted to describe the trends of the experimental gaps reported in Ref. [12] between the $1h_{11/2}$-$1g_{7/2}$ s.p. proton levels in Sn isotopes and the $1i_{13/2}$-$1h_{9/2}$ s.p. neutron levels in the $N = 82$ isotonic chain. Our results are compared with the predictions of other mean-field models containing a tensor force, namely, the SIII-T, SLy5-T, and SAMi-T Skyrme interactions and the D1MTd Gogny interaction. We have also analyzed the evolution of the $1h_{11/2}$, $1g_{7/2}$, and $2d_{3/2}$ neutron s.p. levels in the $N = 51$ isotonic chain. It is found that when the tensor force acts, the energy of the $1g_{7/2}$ s.p. neutron level decreases when the occupancy of the $1g_{9/2}$ proton level grows, in agreement with the predictions of Federman and Pittel [58]. Our calculations show that the SEI predictions qualitatively reproduce the experimental trends along the considered isotopic and isotonic chains, while the agreement with the experiment is deteriorated if the tensor term is not included in SEI. The effects due to the pairing correlations in the presence of the tensor force are discussed in the case of the SIII-T interaction (we have found comparable effects in the case of the D1M and D1MTd Gogny interactions). It is seen that its impact depends on the position of the different s.p. levels, which may be relevant in some cases. It is known that in general the tensor interaction reduces the pairing correlations [59].

In this work we have seen that, by including a short-range tensor term to the standard spin-orbit interaction, one is able to explain in a qualitative way the experimentally observed behavior of some specific energy gaps in the Sn isotopes and in the $N = 82$ and $N = 51$ isotonic chains. But to have a more quantitative explanation, it appears that the tensor and the spin-orbit interactions should be modified, for example, by introducing a finite range in the tensor force and by exploring a more flexible spin-orbit part, which are tasks for future research.

ACKNOWLEDGMENTS

Useful discussions with F. Stancu are warmly acknowledged. P. Bano acknowledges the support from MANF Fellowship of UGC, India. T.R.R. gives sincere thanks to Professor B. Behera for meaningful discussions. M.C. and X.V. were partially supported by Grants No. PID2020-118758GB-I00 and No. CEX2019-000918-M (through the "Unit of Excellence María de Maeztu 2020-2023" award to ICCUB) from the Spanish MCIN/AEI (DOI 10.13039/501100011033).

The work of L.M.R. was partly supported by the Spanish MINECO Grant No. PGC2018-094583-B-I00. M.A. has been partially supported by the Spanish MINECO Grant No. PID2019-104888GB-I00.

[1] M. Stanoiu *et al.*, Phys. Rev. C **69**, 034312 (2004).
[2] B. A. Brown and W. A. Richter, Phys. Rev. C **72**, 057301 (2005).
[3] E. Becheva, T. Suzuki, M. Honma, Y. Utsuno, N. Tsunoda, K. Tsukiyama, and Hjorth-M. Jensen, Phys. Rev. Lett. **96**, 012501 (2006).
[4] C. R. Hoffman *et al.*, Phys. Lett. B **672**, 17 (2009).
[5] K. Tshoo *et al.*, Phys. Rev. Lett. **109**, 022501 (2012).
[6] R. Kanungo, I. Tanihata, and A. Ozawa, Phys. Lett. B **528**, 58 (2002).
[7] M. Rosenbusch *et al.*, Phys. Rev. Lett. **114**, 202501 (2015).
[8] A. Gade *et al.*, Phys. Rev. C **74**, 021302(R) (2006).
[9] F. Wienholtz *et al.*, Nature (London) **498**, 346 (2013).
[10] D. Steppenbeck *et al.*, Nature (London) **502**, 207 (2013).
[11] S. Michimasa *et al.*, Phys. Rev. Lett. **121**, 022506 (2018).
[12] J. P. Schiffer, S. J. Freeman, J. A. Caggiano, C. Deibel, A. Heinz, C. L. Jiang, R. Lewis, A. Parikh, P. D. Parker, K. E. Rehm, S. Sinha, and J. S. Thomas, Phys. Rev. Lett. **92**, 162501 (2004).
[13] L. Gaudefroy, O. Sorlin, D. Beaumel, Y. Blumenfeld, Z. Dombradi, S. Fortier, S. Franchoo, M. Gelin, J. Gibelin, S. Grevy, F. Hammache, F. Ibrahim, K. W. Kemper, K. L. Kratz, S. M. Lukyanov, C. Monrozeau, L. Nalpas, F. Nowacki, A. N. Ostrowski, T. Otsuka, Y. E. Penionzhkevich, J. Piekarewicz, E. C. Pollacco, Roussel-P. Chomaz, E. Rich, J. A. Scarpaci, M. G. S. Laurent, D. Sohler, M. Stanoiu, T. Suzuki, E. Tryggestad, and D. Verney, Phys. Rev. Lett. **97**, 092501 (2006).
[14] G. Colò, H. Sagawa, S. Fracasso, and P. F. Bortignon, Phys. Lett. B **646**, 227 (2007).
[15] T. Otsuka, R. Fujimoto, Y. Utsuno, B. A. Brown, M. Honma, and T. Mizusaki, Phys. Rev. Lett. **87**, 082502 (2001).
[16] T. Otsuka, T. Suzuki, R. Fujimoto, H. Grawe, and Y. Akaishi, Phys. Rev. Lett. **95**, 232502 (2005).
[17] T. Otsuka, T. Suzuki, M. Honma, Y. Utsuno, N. Tsunoda, K. Tsukiyama, and M. Hjorth-Jensen, Phys. Rev. Lett. **104**, 012501 (2010).
[18] W. Rarita and J. Schwinger, Phys. Rev. **59**, 436 (1941); **59**, 556 (1941).
[19] J. M. Blatt and V. F. Weisskopf, *Theoretical Nuclear Physics* (Wiley, New York, 1952).
[20] B. Behera, X. Viñas, M. Bhuyan, T. R. Routray, B. K. Sharma, and S. K. Patra, J. Phys. G **40**, 095105 (2013).
[21] B. Behera, X. Viñas, T. R. Routray, L. M. Robledo, M. Centelles, and S. P. Pattnaik, J. Phys. G **43**, 045115 (2016).
[22] L. Olivier, S. Franchoo, M. Niikura, Z. Vajta, D. Sohler, P. Doornenbal, A. Obertelli, Y. Tsunoda, T. Otsuka, G. Authele *et al.*, Phys. Rev. Lett. **119**, 192501 (2017).
[23] E. Sahin, F. L. Bello Garrote, Y. Tsunoda, T. Otsuka, G. de Angelis, A. Görgen, M. Niikura, S. Nishimura, Z. Y. Xu, H. Baba *et al.*, Phys. Rev. Lett. **118**, 242502 (2017).
[24] T. R. Routray, P. Bano, M. Anguiano, M. Centelles, X. Viñas, and L. M. Robledo, Phys. Rev. C **104**, L011302 (2021)
[25] D. M. Brink and F. Stancu, Phys. Rev. C **97**, 064304 (2018).
[26] S. Shen, G. Colò, and X. Roca-Maza, Phys. Rev. C **99**, 034322 (2019).
[27] M. Anguiano, M. Grasso, G. Co', V. De Donno, and A. M. Lallena, Phys. Rev. C **86**, 054302 (2012).
[28] M. Anguiano, A. M. Lallena, G. Colò, V. De Donno, M. Grasso, and R. N. Bernard, Eur. Phys. J. A **52**, 183 (2016).
[29] M. Anguiano, G. Co', V. De Donno, and A. M. Lallena, Phys. Rev. C **83**, 064306 (2011).
[30] V. B. Soubbotin and X. Viñas, Nucl. Phys. A **665**, 291 (2000).
[31] V. B. Soubbotin, V. I. Tselyaev, and X. Viñas, Phys. Rev. C **67**, 014324 (2003).
[32] B. Behera, T. R. Routray, and R. K. Satpathy, J. Phys. G **24**, 2073 (1998).
[33] G. F. Bertsch and S. Das Gupta, Phys. Rep. **160**, 189 (1988).
[34] C. Gale, G. Bertsch, and S. Das Gupta, Phys. Rev. C **35**, 1666 (1987).
[35] C. Gale, G. M. Welke, M. Prakash, S. J. Lee, and S. Das Gupta, Phys. Rev. C **41**, 1545 (1990).
[36] L. P. Csernai, G. Fai, C. Gale, and E. Osnes, Phys. Rev. C **46**, 736 (1992).
[37] B. Behera, T. R. Routray, and S. K. Tripathy, J. Phys. G **38**, 115104 (2011).
[38] B. Behera, X. Viñas, T. R. Routray, and M. Centelles, J. Phys. G **42**, 045103 (2015).
[39] P. Danielewicz, R. Lacey, and W. G. Lynch, Science **298**, 1592 (2002).
[40] B. Behera, T. R. Routray, and R. K. Satpathy, J. Phys. G **23**, 445 (1997).
[41] F. Sammarruca, Int. J. Mod. Phys. E **19**, 1259 (2010).
[42] R. B. Wiringa, Phys. Rev. C **38**, 2967 (1988).
[43] A. Akmal, V. R. Pandharipande, and D. G. Ravenhall, Phys. Rev. C **58**, 1804 (1998).
[44] B. Behera, T. R. Routray, and S. K. Tripathy, J. Phys. G **36**, 125105 (2009).
[45] T. R. Routray, X. Viñas, D. N. Basu, S. P. Pattnaik, M. Centelles, L. B. Robledo, and B. Behera, J. Phys. G **43**, 105101 (2016).
[46] G. F. Bertsch, W. Loveland, W. Nazarewicz, and P. Talou, J. Phys. G **42**, 077001 (2015).
[47] https://www.nndc.bnl.gov/nudat2/.
[48] S. Malbrunot-Ettenauer, S. Kaufmann, S. Bacca, C. Barbieri, J. Billowes *et al.*, Phys. Rev. Lett. **128**, 022502 (2022).
[49] F. Stancu, D. M. Brink, and H. Flocard, Phys. Lett. B **68**, 108 (1977).
[50] S. Perez-Martin and L. M. Robledo, Phys. Rev. C **78**, 014304 (2008).
[51] L. Bonneau, P. Quentin, and P. Möller, Phys. Rev. C **76**, 024320 (2007).
[52] S. Hilaire and M. Girod, *The AMEDEE Nuclear Structure Database, presented at the International Conference on Nuclear Data for Science and Technology* (2007).
[53] S. Shlomo, V. M. Kolomietz, and G. Colò, Eur. Phys. J. A **30**, 23 (2006).
[54] J. R. Stone, N. J. Stone, and S. A. Moszkowski, Phys. Rev. C **89**, 044316 (2014).
[55] J. Piekarewicz and M. Centelles, Phys. Rev. C **79**, 054311 (2009).
[56] T. Li, U. Garg, Y. Liu, R. Marks, B. K. Nayak, P. V. R. Madhusudhana, M. Fujiwara, H. Hashimoto, K. Kawase, K.

Nakanishi, S. Okumura, M. Yosoi, M. Itoh, M. Ichikawa, R. Matsuo, T. Terazono, M. Uchida, T. Kawabata, H. Akimune, Y. Iwao, T. Murakami, H. Sakaguchi, S. Terashima, Y. Yasuda, J. Zenihiro, and M. N. Harakeh, Phys. Rev. Lett. **99**, 162503 (2007).

[57] Y. Wang, C. Guo, Q. Li, A. Le Févre, Y. Leifels, and W. Trautmann, Phys. Lett. B **778**, 207 (2018).

[58] P. Federman and S. Pittel, Phys. Lett. B **69**, 385 (1977).

[59] M. Anguiano, R. N. Bernard, A. M. Lallena, G. Co', and V. De Donno, Nucl. Phys. A **955**, 181 (2016).